Analytical methods for predicting the response of marine risers, communicated by W.T. Koiter

Proceedings B 85 (4), December 13, 1982

Analytical methods for predicting the response of marine risers

by J.J.H. Brouwers

Koninklijke/Shell Exploratie en Produktie Laboratorium, Rijswijk, the Netherlands

Communicated by Prof. W.T. Koiter at the meeting of May 24, 1982

SUMMARY

A marine riser, which links a floating oil or gas production system to a sea-bed manifold, can be modelled as a tensioned beam, the hydrodynamic transverse forces being described by the relative velocity form of Morison's equation. To analyse the response of the riser to random waves and floater motions, a number of characteristic regions has been identified along the riser. For each of these regions, the riser differential equation is reduced to an approximate form and analytical solutions, in terms of known time- and position-dependent functions, are given. The solutions hold asymptotically for slender (tension-dominated) risers in deep water and compare favourably with numerical simulation results for a typical riser.

INTRODUCTION

Floating production systems tend to form an attractive possibility for the development of offshore oil and gas fields, particularly in deep water. A critical element in these systems is the riser, which links the floating unit (e.g. a vessel or a semi-submersible) to the sea-bed manifold (see fig. 1). The main purpose of the riser is to conduct fluid (oil, gas) from the sea-bed to the surface and vice versa.

Various loads are imposed on the riser, including loads induced by waves, currents and floater motions. Some of these, i.e. waves and floater motions, vary randomly with time. Riser response must therefore be treated as a random variable, characterised by probability distributions. Realistic prediction of these distributions is important for assessing design parameters such as expected fatigue damage and expected extreme response.

Two types of riser analysis are commonly employed, viz. analysis in the frequency domain using spectral analysis techniques (Tucker and Murtha, 1973, Kirk et al., 1979, Krolikowsky and Gay, 1980) and analysis in the time domain using numerical simulation techniques (Sexton and Agbezuge, 1976, Harper, 1979). The first method yields valid solutions for linear systems with Gaussian excitation, where response is also Gaussian. In riser analysis,

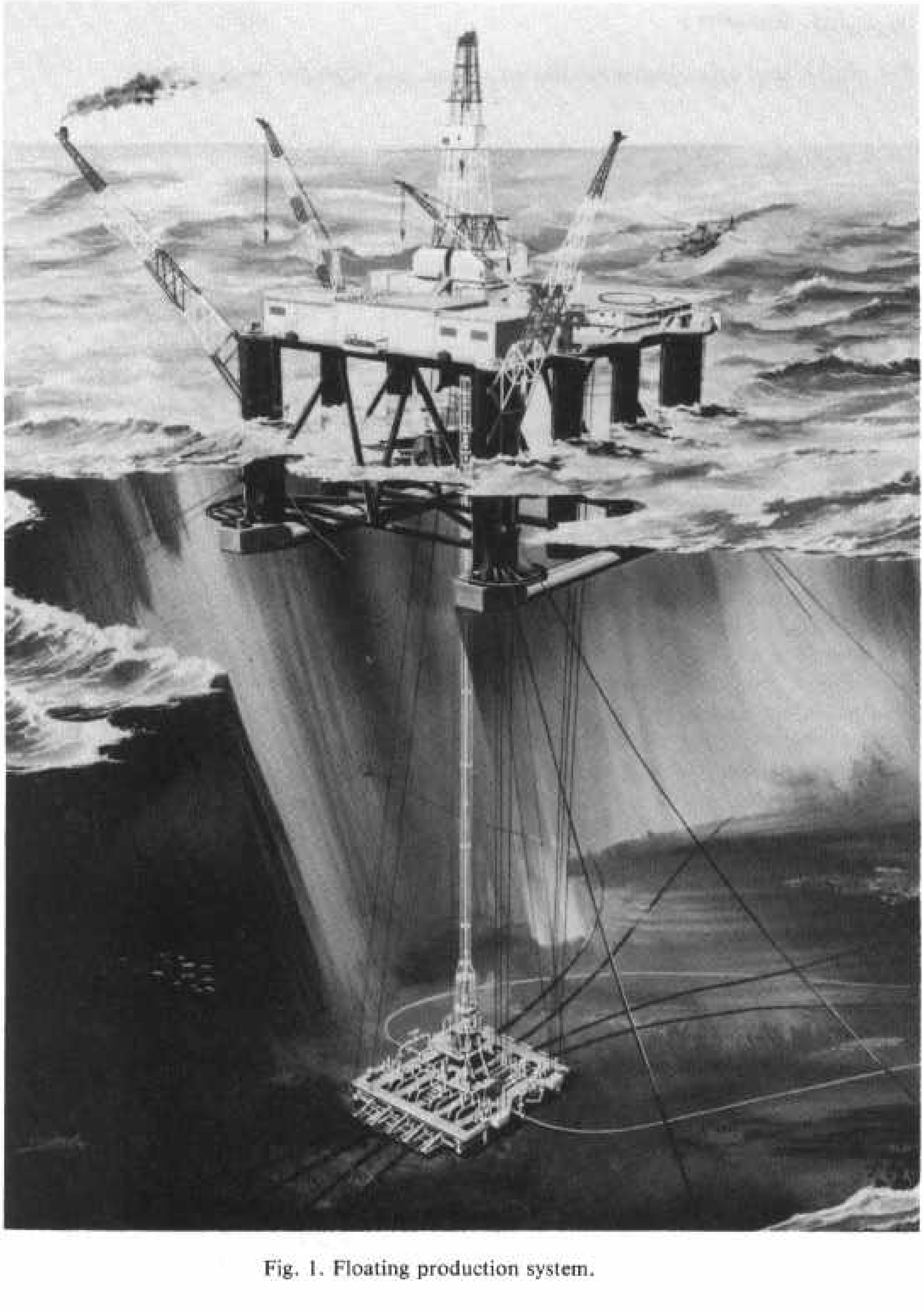

Fig. 1. Floating production system.

however, it is often necessary to describe the system in a non-linear manner, using a form of Morison's equation for the hydrodynamic force. Spectral analysis techniques then only yield approximate results and are unable to predict deviations from the Gaussian form caused by non-linearities.

The second method, i.e. numerical time-domain simulation, enables the effect of non-linear elements on response distributions to be determined. The solution routine, however, is rather elaborate and time-consuming. Results are generally limited to those obtained from short-term simulations of typical cases. The solution method is less suitable for obtaining information on extreme and long-term statistics or for identifying general trends in riser response.

In this paper an alternative method is described for analysing non-linear riser behaviour in random seas. Rather than numerically, riser response to random waves and floater motions is investigated analytically. The analytical approach involves identification of characteristic regions along the riser. For each of these regions, the riser differential equation is reduced to an approximate form and analytical solutions, in terms of known functions, are given. A comparison with numerical simulation results for a typical riser is also made.

BASIC EQUATIONS

In general, a marine riser can be represented as an almost straight, vertical, tensioned beam, which is subject to an axially distributed two-dimensional transverse force $\boldsymbol{F}(z, t)$. For axi-symmetric riser configurations, the two-dimensional response of the riser can be described by the differential equation

$$(1) \qquad EI\frac{\partial^4 \boldsymbol{x}}{\partial z^4} - \frac{\partial}{\partial z}\left(T_r(z)\frac{\partial \boldsymbol{x}}{\partial z}\right) + m\frac{\partial^2 \boldsymbol{x}}{\partial t^2} = \boldsymbol{F},$$

where

$\boldsymbol{x}(z, t)$ = two-dimensional horizontal deflection,
z = vertical distance from riser base,
t = time,
E = modulus of elasticity,
I = moment of inertia,
$T_r(z)$ = riser tension ($T_r > 0$),
m = mass per unit length,
$\boldsymbol{F}(z, t)$ = external force per unit length.

The bottom end of the riser is assumed to be fixed to the base,

$$(2) \qquad \boldsymbol{x} = 0 \quad \text{at } z = 0,$$

and subject to rotational constraint according to

$$(3) \qquad EI\frac{\partial^2 \boldsymbol{x}}{\partial z^2} = C_b\frac{\partial \boldsymbol{x}}{\partial z} \quad \text{at } z = 0,$$

where C_b is the rotational stiffness of the riser base. At the top, the riser is assumed to be connected by a hinge to a floating structure, expressed as

(4) $\quad \boldsymbol{x}=\boldsymbol{v} \quad \text{at } z=L,$

(5) $\quad EI\dfrac{\partial^2 \boldsymbol{x}}{\partial z^2}=0 \quad \text{at } z=L,$

where $\boldsymbol{v}(t)$ is the time-dependent horizontal displacement of the floating structure and L is the length of the riser. The configuration is shown in fig. 2. The derivation of riser differential equation (1) is illustrated in fig. 3.

The terms on the left-hand side of equation (1) represent bending forces, $EI(\partial^4/\partial z^4)\boldsymbol{x}$, tension forces, $(\partial/\partial z)(T_r(\partial/\partial z)\boldsymbol{x})$, and inertia forces, $m(\partial^2/\partial t^2)\boldsymbol{x}$,

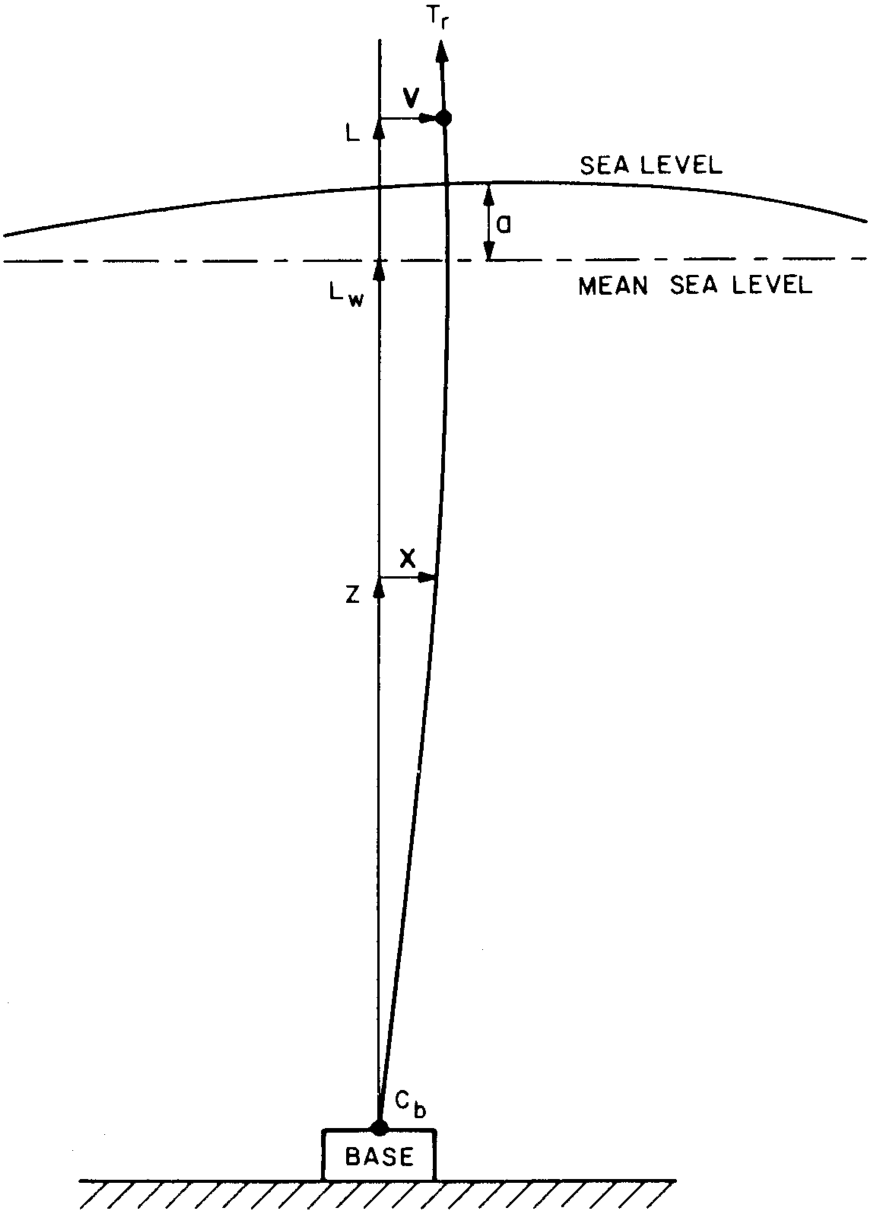

Fig. 2. Riser configuration.

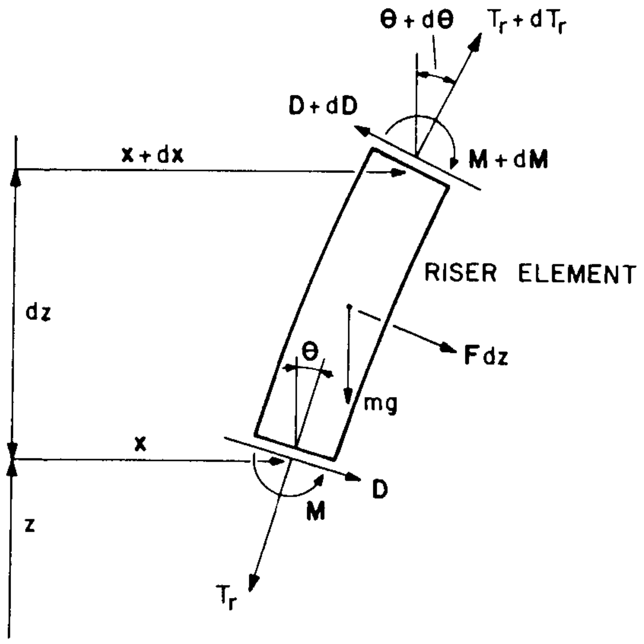

NEWTON'S SECOND LAW IN HORIZONTAL DIRECTION (EXCLUDING NON-LINEAR TERMS):

$$-dD + d(T_r\,\theta) + F\,dz - D_m dz = m\frac{\delta^2 x}{\delta t^2}\,dz. \qquad \text{(A)}$$

EQUILIBRIUM OF MOMENTS (EXCLUDING NON-LINEAR TERMS):

$$dM = D\,dz \qquad \text{(B)}$$

BERNOULLI-EULER EQUATION:

$$M = EI\frac{\delta^2 x}{\delta z^2} \qquad \text{(C)}$$

GEOMETRICAL RELATION:

$$\theta = \frac{\delta x}{\delta z} \qquad \text{(D)}$$

SUBSTITUTING (B), (C) AND (D) INTO (A) YIELDS DIFFERENTIAL EQUATION (1)

Fig. 3. Derivation of riser differential equation.

respectively. These forces are balanced by the transverse force $\boldsymbol{F}(z, t)$, which is described as

(6) $$\boldsymbol{F} = \boldsymbol{F}_H H(L_w + a(t) - z),$$

where $\boldsymbol{F}_H(z, t)$ is the hydrodynamic force exerted by the water and $H(L_w + a(t) - z)$ is Heaviside's unit function. This function models the sea level according to

(7a), (7b) $$H(L_w + a(t) - z) = \begin{cases} 1 \text{ for } z < L_w + a(t) \\ 0 \text{ for } z > L_w + a(t) \end{cases}$$

where L_w is the mean sea level as measured from the riser base and $a(t)$ is the (wind-generated) surface elevation as measured from the mean sea level (see fig. 2).

Ignoring effects such as vortex induced vibrations, the hydrodynamic force is commonly described by the 'relative velocity' form of Morison's equation:

(8) $$\boldsymbol{F}_H = \boldsymbol{F}_I + \boldsymbol{F}_D,$$

where $\boldsymbol{F}_I(z, t)$ is the inertia force, defined by

(9) $$\boldsymbol{F}_I = \tfrac{1}{4}\varrho\pi d^2 C_m \frac{\partial^2 \boldsymbol{w}}{\partial t^2} - \tfrac{1}{4}\varrho\pi d^2 C_A \frac{\partial^2 \boldsymbol{x}}{\partial t^2},$$

and $\boldsymbol{F}_D(z, t)$ is the drag force, defined by

(10) $$\boldsymbol{F}_D = \tfrac{1}{2}\varrho d C_D \left(\frac{\partial \boldsymbol{w}}{\partial t} + \boldsymbol{u}_c - \frac{\partial \boldsymbol{x}}{\partial t}\right)\left|\frac{\partial \boldsymbol{w}}{\partial t} + \boldsymbol{u}_c - \frac{\partial \boldsymbol{x}}{\partial t}\right|.$$

In the above equations

- ϱ = water density,
- d = riser diameter (or equivalent diameter),
- C_M = inertia coefficient ($C_M \approx 2$),
- C_A = added mass coefficient ($C_A \approx 1$),
- C_D = drag coefficient ($C_D \approx 1$),
- $\boldsymbol{w}(z, t)$ = horizontal displacement of water particles due to (wind-generated) surface waves,
- $\boldsymbol{u}_c(z)$ = horizontal current velocities (e.g. tidal currents).

The larger value for C_M as compared to that for C_A in the expression for the inertia force represents additional force due to pressure gradients associated with acceleration of the fluid: see Batchelor (1967), p. 409. The description of the drag force is based on the assumption that drag forces are due to pressure differences caused by boundary layer separation from the riser surface. The force can then be taken to be quadratically dependent on relative velocities. For a discussion on Morison's equation, reference is made to Hogben et al. (1977) and Sarpkaya (1981).

REGIONS OF RISER RESPONSE

For slender (tension-dominated) risers in deep water, a distinction can be made between three regions: a wave-active zone at the top, a boundary layer at the bottom and a riser main section in between (see fig. 4).

In the wave-active zone, the riser is exposed to direct wave loading due to wave-induced water particle motions $\boldsymbol{w}(z, t)$. According to wave theory (Kinsman, 1965), $\boldsymbol{w}(z, t)$ decays exponentially in magnitude from mean sea level over a length λ_w, given by

(11) $$\lambda_w = g/\omega_a^2,$$

where g is the gravitational acceleration and ω_a the characteristic (mean)

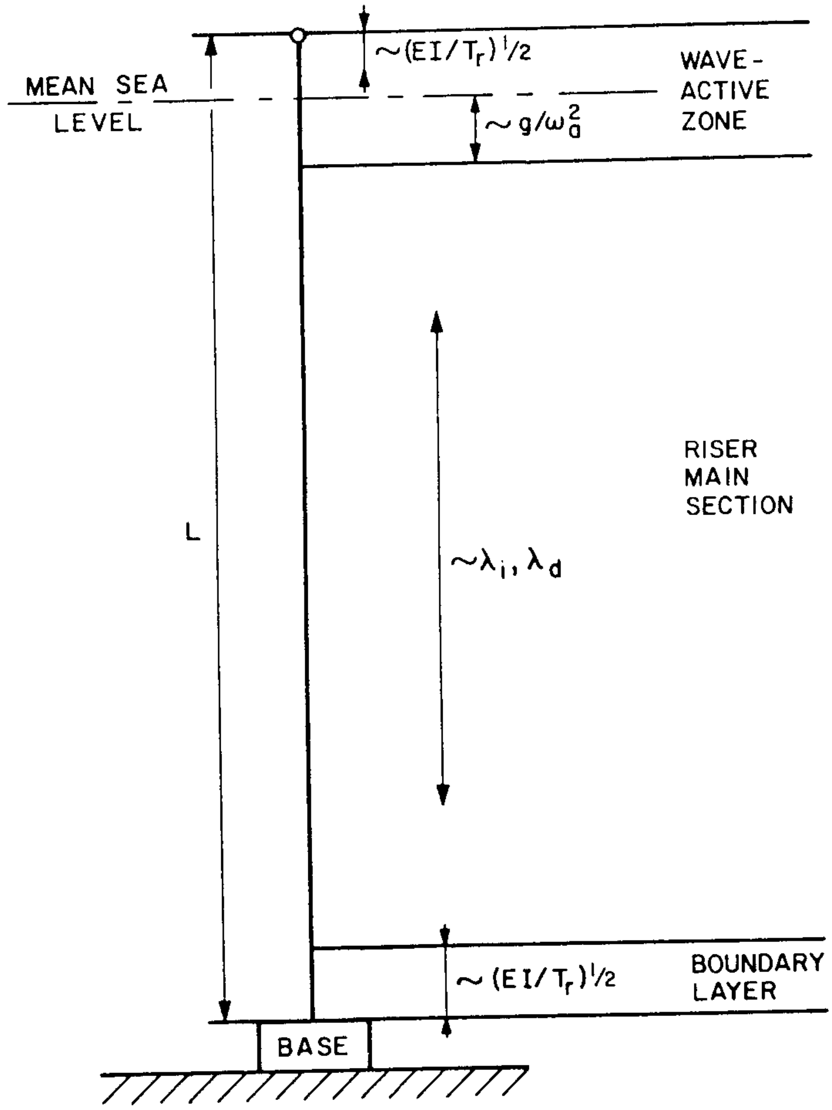

Fig. 4. Regions of response.

frequency of the sea surface elevation. In practice, g/ω_a^2 is 10–40 m. The height of the riser above mean sea level is, in general, of the same order of magnitude. The region extending from riser top to a distance $\sim\lambda_w$ below mean sea level is referred to as the 'wave-active zone'. Below this region, wave-induced water particle displacements $\boldsymbol{w}(z,t)$ and forces associated with $\boldsymbol{w}(z,t)$ (see eqs. 9 and 10) can be disregarded.

The boundary layer at the bottom extends over a length $\sim\lambda_b$, where

(12) $\lambda_b=(EI/T_r)^{\frac{1}{2}}$.

As can be verified from riser differential equation (1), $(EI/T_r)^{\frac{1}{2}}$ is the characteristic length over which response must vary for the tension and bending forces to be of equal order of magnitude. If the response varies over a length substantially exceeding λ_b, tension forces will dominate bending forces. For conventional small-diameter risers ($d\leq 0.5$ m), λ_b will, in general, not exceed 10 m. This length is, in general, small compared to the length over which the response varies in the main portion of the riser, which is discussed in the next paragraphs. Hence, in most parts of small-diameter risers, the effects of bending forces can be disregarded. Bending forces, i.e. the highest axial derivatives in the differential equation, are then only important in local regions of length $\sim \lambda_b$ at any discontinuity in the riser, with the top and bottom ends as special cases (see fig. 4).

In the riser main section, bending forces and hydrodynamic forces due to wave-induced water particle motions can be disregarded. In this region, the riser can be represented as an entirely submerged tensioned string, subject to transverse displacement excitation at one end, and fixed at the other. The characteristic length over which the response varies can be indicated by λ_m, defined as the minimum of the 'dynamic' lengths λ_i and λ_d, and riser length L: i.e.,

(13) $$\lambda_m = \min.[\lambda_i, \lambda_d, L],$$

where

(14) $$\lambda_i = \pi T_r^{\frac{1}{2}}(m + m_A)^{-\frac{1}{2}}\omega_a^{-1}$$

and

(15) $$\lambda_d = \lambda_i \delta^{-\frac{1}{2}}.$$

In the above equations, $m_A = \frac{1}{4}\varrho\pi d^2 C_A$ is added mass of the water per unit length and δ is drag-inertia parameter, to be defined below.

The length λ_i, as defined by equation (14), corresponds to half the wave length of a lightly damped tensioned string. Here the response length is determined by a balance between the tension and inertia forces in riser differential equation (1). For some typical values of riser parameters it has been found that λ_i is between 150 and 300 m.

In the case of large damping, the dynamic response length can well be determined by a balance between tension and drag forces. The characteristic length of the response is then smaller than λ_i and can be related to λ_i, as indicated in equation (15). Here, δ represents the ratio between drag forces and inertia forces. For low current velocities, i.e. where $\boldsymbol{u}_c$ is small as compared to riser velocity $(\partial/\partial t)\boldsymbol{x}$, this ratio can be expressed as

(16) $$\delta = \frac{\frac{1}{2}\varrho d C_D \sigma}{m + m_A},$$

where σ is the typical value for riser deflection, e.g. standard deviation of floater displacement. For high current velocities, i.e. $|\boldsymbol{u}_c| \gg |(\partial/\partial t)\boldsymbol{x}|$, the dynamic component of the drag force is primarily given by cross-products of $\boldsymbol{u}_c$ with $(\partial/\partial t)\boldsymbol{x}$: see equation (10). An appropriate drag-inertia parameter is then given by equation (16), if σ is replaced by $\omega_a^{-1}|\boldsymbol{u}_c|$.

The smaller of the lengths λ_i and λ_d is representative of the length over which the response varies in the main section, as long as this length is of the same order of magnitude as the riser length L, or smaller. If λ_i and λ_d are much larger than L, however, the response is of a quasi-static nature. Restoring forces then dominate inertia and drag forces and the response in the main section will vary over the length L. Note that also in local response regions (wave-active zone, boundary layer at the bottom), whose lengths are much smaller than the dynamic lengths λ_i and λ_d, response will be of quasi-static nature.

SOLUTION PROCEDURE

To calculate riser response in the wave-active zone at the top, the boundary layer at the bottom, and the riser main section, use can be made of a formal mathematical procedure which consists in applying perturbation techniques and methods of matched asymptotic expansions (Van Dyke, 1964). The solution procedure involves reduction of the riser differential equation to an approximate form by expressing the solution as a perturbation expansion in powers of a small dimensionless parameter. For the wave-active zone at the top and the boundary layer at the bottom, the small dimensionless parameter is given by the ratio of the characteristic lengths λ_w/λ_m and λ_b/λ_m, respectively; the expansion for the main section involves both λ_w/λ_m and λ_b/λ_m. The requirement that the solutions of the simplified differential equations of each region must join in a prescribed manner is known as the matching principle (Van Dyke, 1964). It connects the solutions of each region and leads to a consistent description of the response over the entire riser.

In the subsequent paragraphs a less formal approach will be adopted to calculate riser response. Rather than introducing extensive perturbation schemes, the riser differential equation is directly reduced to an approximate form by neglecting those terms that are small according to the analysis given in the previous section. Matching is accomplished by employing heuristic arguments such as 'solutions for the boundary layer at the bottom should remain finite as the boundary layer coordinate tends to infinity'. The resulting solutions are equal to the descriptions of the first term of the perturbation expensions as obtained from perturbation techniques and matched asymptotic expansion procedures. The given solutions and descriptions are thus asymptotically valid in the limit of $\lambda_w/\lambda_m \to 0$ and $\lambda_b/\lambda_m \to 0$, and can be expected to be accurate if

(17) $\lambda_w \ll \lambda_m$ and $\lambda_b \ll \lambda_m$,

i.e. if the characteristic lengths of the wave active zone (cf. eq. 11) and the boundary layer at the bottom (cf. eq. 12) are much smaller than the characteristic length over which response varies in the main section (cf. eqs. 13–16).

SOLUTIONS FOR THE WAVE-ACTIVE ZONE

For most practical cases, λ_w is much smaller than the dynamic lengths λ_i and λ_d. Response in the wave-active zone is then of a quasi-static nature and both the inertia term and fluid loading term can be disregarded as a first approximation for evaluating $\boldsymbol{x}$. Displacement response in the wave active zone is thus primarily governed by a balance between the tension forces and bending forces only. Assuming that the tension $T_r(z)$ is almost constant over the wave-active zone, riser differential equation (1) can then be approximated by

$$EI\frac{\partial^4 \boldsymbol{x}}{\partial z^4} - T_r\frac{\partial^2 \boldsymbol{x}}{\partial z^2} = 0. \tag{18}$$

The solution of this equation, which satisfies the boundary conditions imposed at the riser top (equations 4 and 5) and which remains finite as $(L-z)\lambda_w^{-1} \to \infty$, i.e. when entering into the riser main section, is

$$\boldsymbol{x}(z,t) = \boldsymbol{v}(t). \tag{19}$$

To first order, the horizontal deflection of the riser in the wave-active zone is thus equal to the horizontal deflection of the floater imposed at the top. The effect of direct wave loading on horizontal deflection can be shown to be $O(|\boldsymbol{w}|\lambda_w^2/\lambda_m^2)$, where $|\boldsymbol{w}|$ is the characteristic magnitude of wave-induced horizontal water particle displacement: e.g. standard deviation of sea-surface elevation. In general, this effect is small (because $\lambda_w^2/\lambda_m^2 \ll 1$).

Descriptions for the bending moment in the wave-active zone can be derived by substituting the above solution for deflection into the expressions for the inertia forces and damping forces of riser differential equation (1). This gives the equation

$$EI\frac{\partial^4 \boldsymbol{x}}{\partial z^4} - T_r\frac{\partial^2 \boldsymbol{x}}{\partial z^2} = \boldsymbol{F}_s, \tag{20}$$

or, in terms of the bending moment $\boldsymbol{M}(z,t)$ defined by

$$\boldsymbol{M} = EI\frac{\partial^2 \boldsymbol{x}}{\partial z^2}, \tag{21}$$

the equation

$$\frac{\partial^2 \boldsymbol{M}}{\partial z^2} - (T_r/EI)\boldsymbol{M} = \boldsymbol{F}_s. \tag{22}$$

Here, $\boldsymbol{F}_s(z,t)$ is the sum of the inertia forces and hydrodynamic forces acting on the riser when the horizontal displacement of the riser is equal to the horizontal displacement of the vessel $\boldsymbol{v}(t)$:

$$\boldsymbol{F}_s = -m\frac{d^2\boldsymbol{v}}{dt^2} + \boldsymbol{F}_{\boldsymbol{x}=\boldsymbol{v}}, \tag{23}$$

where $\boldsymbol{F}(z,t)$ is defined by equations (6)–(10).

The solution of equation (22), which satisfies the boundary condition imposed at the top (equation 5) and which remains finite as $(L-z)\lambda_w^{-1} \to \infty$, can be obtained using Laplace transformation techniques. This solution is given by

$$\text{(24)} \quad \begin{cases} \boldsymbol{M}(z,t) = \lambda_b \int_z^L \boldsymbol{F}_s(x,t) \sinh \{(x-z)\lambda_b^{-1}\} dx \\ \qquad - \lambda_b \sinh \{(L-z)\lambda_b^{-1}\} \int_0^L \boldsymbol{F}_s(x,t) \exp \{(x-L)\lambda_b^{-1}\} dx, \end{cases}$$

where λ_b is the 'boundary layer' length defined by equation (12).

According to the above solution, the bending moment in the wave-active zone is linearly and quasi-statically related to the inertia and hydrodynamic force $\boldsymbol{F}_s(z,t)$ acting on the riser when the riser moves with the floater. The governing probability distributions of bending moment, such as the distribution of instantaneous values and peak values, can therefore be expected to be similar to those of the force $\boldsymbol{F}_s(z,t)$. Because of the nonlinear elements in the description of the force (cf. equations 6–10), for Gaussian wave-induced water particle displacements and floater motions, these probability distributions will be different from those known for linear Gaussian processes. To calculate these distributions, use can be made of methods of nonlinear transformation of random variables. These methods have been widely used in the evaluation of the wave force on a fixed pile (Pierson and Holmes, 1965, Borgman, 1972, Tung, 1974, Tickell, 1977, Moe and Crandall, 1978). Extension of these methods to equation (24) is possible and enables determination of the important statistic parameters of bending moment response, such as standard deviation (= root-mean square value in the case of zero-mean response), expected extreme response (= expected value of largest peak in a stationary sea-state of approx. 3 hours) and expected fatigue damage (= expected value of fatigue damage associated with randomly varying bending stress).

To illustrate the analogy between the expressions for bending moment in the wave-active zone and wave force on a fixed pile, consider the case that floater motions and current are small and can be disregarded. Furthermore, assume that the fluctuation of the sea level in the expression for the hydrodynamic force (cf. equation 6) can be neglected. This assumption can be shown to be justified when the standard deviation of sea surface elevation is much smaller than the boundary layer distance λ_b. For a unidirectional and narrow-band representation of wave-induced water particle motions as given by Borgman (1972), the expression for bending moment given by equation (24) can then be reduced to

$$\text{(25)} \quad M(x,t) = -\lambda_b^2\{\tfrac{1}{4}\varrho\pi d^2 C_M \alpha(x)\ddot{w}_s(t) + \tfrac{1}{2}\varrho d C_D \beta(x)\dot{w}_s(t)\,|\,\dot{w}_s(t)\,|\,\}.$$

Here, x is the distance above mean sea level, $w_s(t)$ is the wave-induced water particle displacement at mean sea level (apart from a phase lack of $\pi/2$, $w_s(t)$ is equal to sea-surface elevation) and dots denote the differentiation with respect to time. The x-dependent constants $\alpha(x)$ and $\beta(x)$ are defined by:

$$\text{(26a)} \quad \begin{cases} \alpha(x) = \tfrac{1}{2}(1+\lambda_b/\lambda_w)^{-1}\{\exp(-x/\lambda_b) - \exp((x-2L_1)/\lambda_b)\}, \\ \beta(x) = (1+2\lambda_b/\lambda_w)^{-1}(1+\lambda_b/\lambda_w)\alpha(x), \\ \qquad \text{for } x>0 \text{ (above mean sea level)}, \end{cases}$$

and

$$
(26b)\quad \begin{cases} \alpha(x) = \frac{1}{2}(1+\lambda_b/\lambda_w)^{-1}\{\exp(x/\lambda_w) - \exp((x-2L_1)/\lambda_b)\} \\ \qquad + \frac{1}{2}(1-\lambda_b/\lambda_w)^{-1}\{\exp(x/\lambda_w) - \exp(x/\lambda_b)\}, \\ \beta(x) = \frac{1}{2}(1+2\lambda_b/\lambda_w)^{-1}\{\exp(2x/\lambda_w) - \exp((x-2L_1)/\lambda_b)\} \\ \qquad + \frac{1}{2}(1-2\lambda_b/\lambda_w)^{-1}\{\exp(2x/\lambda_w) - \exp(x/\lambda_b)\}, \\ \qquad \text{for } x<0 \text{ (below mean sea level).} \end{cases}
$$

In the above equations, λ_w is the length of wave-induced water particle displacements, defined by equation (11), and L_1 is the height of the riser above mean sea level.

Apart from some multiplicative constants, equation (25) is equal to Morison's equation for the wave force on a fixed pile. Values for the relevant statistical parameters of bending moment response are thus directly obtainable from the solutions given for the wave force on a fixed pile: e.g. see Borgman (1972). An illustration of the results thus obtained for the vertical distribution of standard deviation of bending moment will be given in the comparison with numerical simulation results at the end of this paper.

SOLUTIONS FOR THE BOUNDARY LAYER AT THE BOTTOM

For tension-dominated risers, λ_b is much smaller than the dynamic lengths λ_i and λ_d. Hence, in the boundary layer at the bottom, inertia forces and damping forces are small. Assuming that the variation of riser tension $T_r(z)$ over the boundary layer is small, riser differential equation (1) can then be approximated by

$$
(27)\qquad EI\frac{\partial^4 \boldsymbol{x}}{\partial z^4} - T_r\frac{\partial^2 \boldsymbol{x}}{\partial z^2} = 0.
$$

In terms of the 'boundary layer' length λ_b, defined by equation (12), and in terms of the riser angle $\theta(z,t)$, defined by

$$
(28)\qquad \theta = \frac{\partial \boldsymbol{x}}{\partial z},
$$

equation (32) can also be written as

$$
(29)\qquad \lambda_b^2\frac{\partial^3\theta}{\partial z^3} - \frac{\partial\theta}{\partial z} = 0.
$$

The three basic solutions of equation (29) are

$$
(30)\qquad \theta(z,t) = \text{constant } (z),\ \exp(-z/\lambda_b),\ \exp(+z/\lambda_b).
$$

For $z/\lambda_b \to \infty$, these solutions should match the value of the angle at the bottom of the riser main section, denoted by $\theta_m(o,t)$. Furthermore, for $z=0$ the above solutions must satisfy the boundary conditions imposed at the riser base (cf.

equation 3). The solution for riser angle in the boundary layer at the bottom is then found to be

$$\theta(z,t)=\theta_m(o,t)\left[1-\left(1+\frac{EI}{C_b\lambda_b}\right)^{-1}\exp\left(-z/\lambda_b\right)\right], \tag{31}$$

while for the bending moment we can write

$$\boldsymbol{M}(z,t)=EI\theta_m(o,t)\lambda_b^{-1}\left(1+\frac{EI}{C_b\lambda_b}\right)^{-1}\exp\left(-z/\lambda_b\right). \tag{32}$$

From the above solutions it can also be verified that the deflection in the boundary layer at the bottom is small and only $O(\lambda_b/\lambda_m)$ compared to the deflection in the riser main section.

From solutions (31) and (32) it is noted that the time-domain behaviour of the angle and bending moment in the boundary layer at the bottom is equal to the (random) time-domain behaviour of the angle at the bottom of the riser main section. The relevant probability distributions of response variables in the boundary layer at the bottom are thus of the same form as those of the angle at the bottom of the main section.

From solutions (32) it is also noted that the rotational constraint C_b imposed at the riser base results in an exponential increase of the bending moment as $z/\lambda_b \to 0$. At $z=0$, we have

$$\boldsymbol{M}(o,t)=EI\theta_m(o,t)\lambda_b^{-1}\left(1+\frac{EI}{C_b\lambda_b}\right)^{-1}. \tag{33}$$

According to this result, the bending moment at $z=0$ increases with increasing rotational stiffness of the riser base C_b and reaches a maximum, equal to

$$\boldsymbol{M}(o,t)=EI\theta_m(o,t)\lambda_b^{-1}, \tag{34}$$

when $C_b\lambda_b \gg EI$. This maximum value is equal to the value obtained in the case of a clamped bottom end. The bottom end thus behaves as a clamped end for rotational stiffnesses of the riser base $C_b \gg EI/\lambda_b$.

SOLUTIONS FOR THE RISER MAIN SECTION

In the riser main section, the effects of wave-induced water particle displacements and bending stiffness can be disregarded. For calculating the response in the main section, riser differential equation (1) can thus be approximated by

$$-\frac{\partial}{\partial z}\left(T_r(z)\,\frac{\partial \boldsymbol{x}}{\partial z}\right)+(m+\tfrac{1}{4}\varrho\pi d^2 C_A)\,\frac{\partial^2 \boldsymbol{x}}{\partial t^2}+\boldsymbol{F}_d\left(\frac{\partial \boldsymbol{x}}{\partial t}\right)=0, \tag{35}$$

where $F_d(\partial \boldsymbol{x}/\partial t)$ is the damping force due to fluid drag:

$$F_d\left(\frac{\partial \boldsymbol{x}}{\partial t}\right)=\tfrac{1}{2}\varrho d C_D\left|\frac{\partial \boldsymbol{x}}{\partial t}-\boldsymbol{u}_c\right|\left(\frac{\partial \boldsymbol{x}}{\partial t}-\boldsymbol{u}_c\right). \tag{36}$$

The boundary conditions for the above second-order differential equation follow from matching to the solutions found for the wave-active zone and the boundary layer at the bottom, respectively. As indicated in the previous section, changes in the horizontal deflection over the boundary layer at the bottom are small. Furthermore, changes in deflection over the wave-active zone are $O(|\boldsymbol{w}|\lambda_w^2/\lambda_m^2)$ and are also assumed to be small (compared to floater displacement). The deflections to be prescribed for differential equation (35) can then be taken to be the sames as those prescribed at riser top and bottom:

(37) $\boldsymbol{x}=\boldsymbol{v}$ at $z=L$,

(38) $\boldsymbol{x}=0$ at $z=0$.

In the particular case of small floater displacement so that $|\boldsymbol{v}| \sim |\boldsymbol{w}|\lambda_w^2/\lambda_m^2$ or less, however, an additional displacement due to wave forces has to be included in boundary condition (37). This displacement is equal to the change in horizontal deflection over the wave-active zone due to wave forces and can be described as

$$T_r^{-1}\int_0^L\int_0^z \boldsymbol{F}_{\boldsymbol{x}=0}\,dz\,dz$$

where $\boldsymbol{F}_{\boldsymbol{x}=0}$ is the hydrodynamic force for zero riser deflection (cf. eqs. 6–10).

A large response in the riser main section can be expected to occur when the damping force is small and when the power density of random floater motion $\boldsymbol{v}(t)$ is such that the riser is also excited at one of its natural frequencies. The solution can then be expressed as the sum of a quasi-static component $\boldsymbol{x}_s(z,t)$ and a dynamic component $\boldsymbol{x}_d(z,t)$:

(39) $\boldsymbol{x}=\boldsymbol{x}_s+\boldsymbol{x}_d.$

The quasi-static component represents the static deflection of the riser due to floater displacement imposed at the top:

(40) $\boldsymbol{x}_s(z,t)=\boldsymbol{v}(t)s(z),$

where

(41) $$s(z)=\int_0^z T_r^{-1}(z)dz\Big/\int_0^L T_r^{-1}(z)dz$$

is the static deflection of the riser for unit deflection imposed at the top. For constant riser tension $T_r(z)$ with respect to z, $s(z)$ reduces to a linear function of z: i.e. $s(z)=z/L$.

The dynamic component $\boldsymbol{x}_d(z,t)$ of the solution represents the resonance response generated by the inertia forces acting on the riser, when the riser moves according to the quasi-static solution. The governing differential equation and boundary conditions for this component can be obtained by substituting equations (39)–(41) into (35)–(38). Neglecting damping forces due to quasi-static riser velocities, it is then found that

(42) $$-\frac{\partial}{\partial z}\left(T_r(z)\frac{\partial \boldsymbol{x}_d}{\partial z}\right)+(m+\tfrac{1}{4}\varrho\pi d^2C_A)\frac{\partial^2\boldsymbol{x}_d}{\partial t^2}+\boldsymbol{F}_d\left(\frac{\partial \boldsymbol{x}_d}{\partial t}\right)=\boldsymbol{F}_e,$$

(43) $\boldsymbol{x}_d = 0$ at $z = 0$ and $z = L$,

where the excitation force $\boldsymbol{F}_e(z, t)$ is given by

(44) $$\boldsymbol{F}_e = -(m + \tfrac{1}{4}\varrho\pi d^2 C_A)s(z)\,\frac{d^2\boldsymbol{v}(t)}{dt^2}.$$

Solutions of equations (42)-(44) can be obtained when the damping is small and excitation occurs predominantly at one of the natural frequencies of the riser (Brouwers, 1982). In this case, the riser will respond predominantly in the corresponding natural mode $x_n(z)$:

(45) $$\boldsymbol{x}_d(z, t) = \boldsymbol{a}_n(t)x_n(z).$$

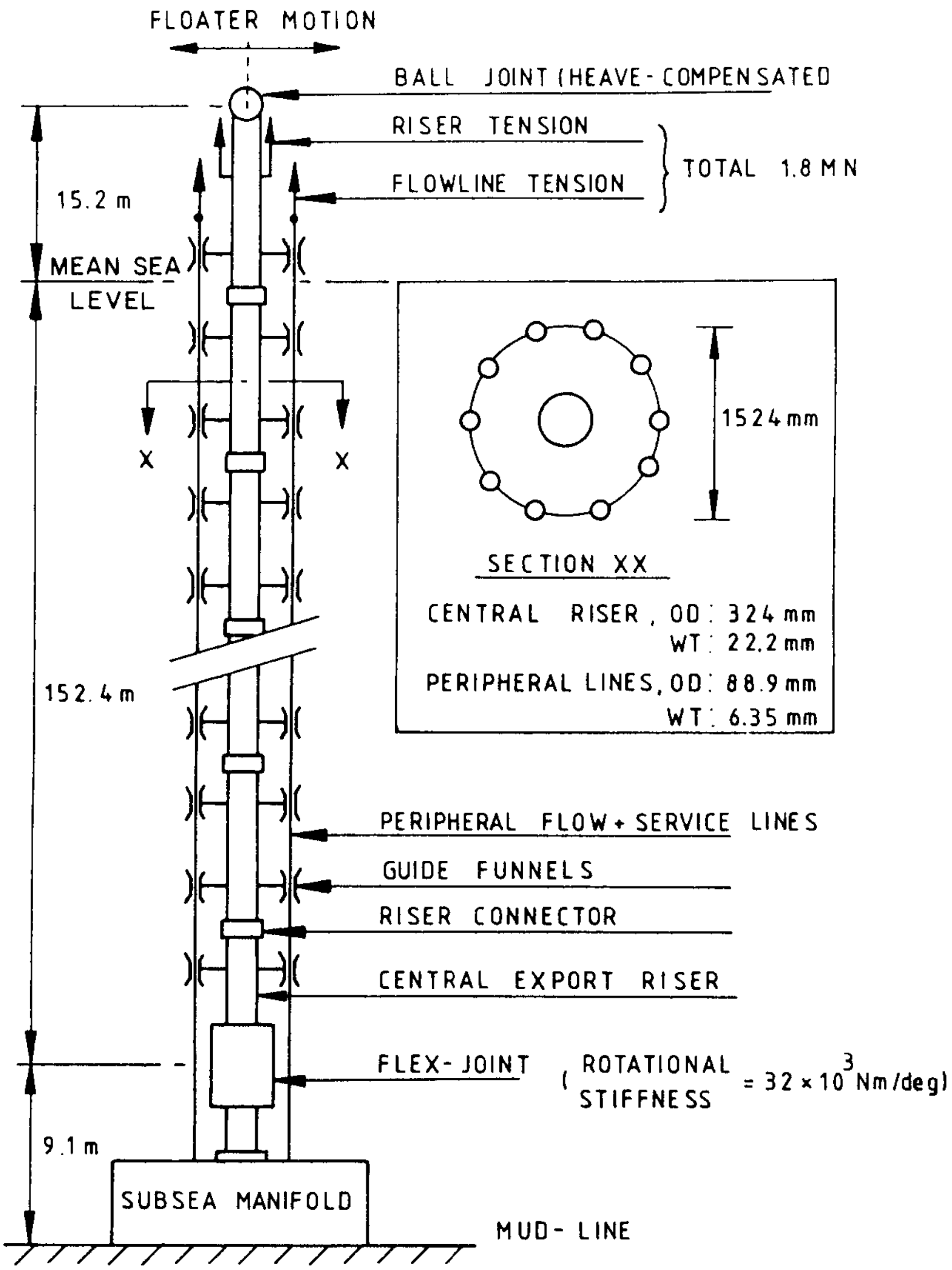

Fig. 5. Multibore production riser.

The amplitude of this mode $a_n(t)$ can be described by a differential equation which is analogous to that of a non-linearly damped system with a single degree of freedom. Closed-form solutions for this problem, in terms of non-Gaussian probability distributions and associated statistical quantities such as standard deviation, expected extreme response and expected fatigue damage, have been given by Brouwers (1982).

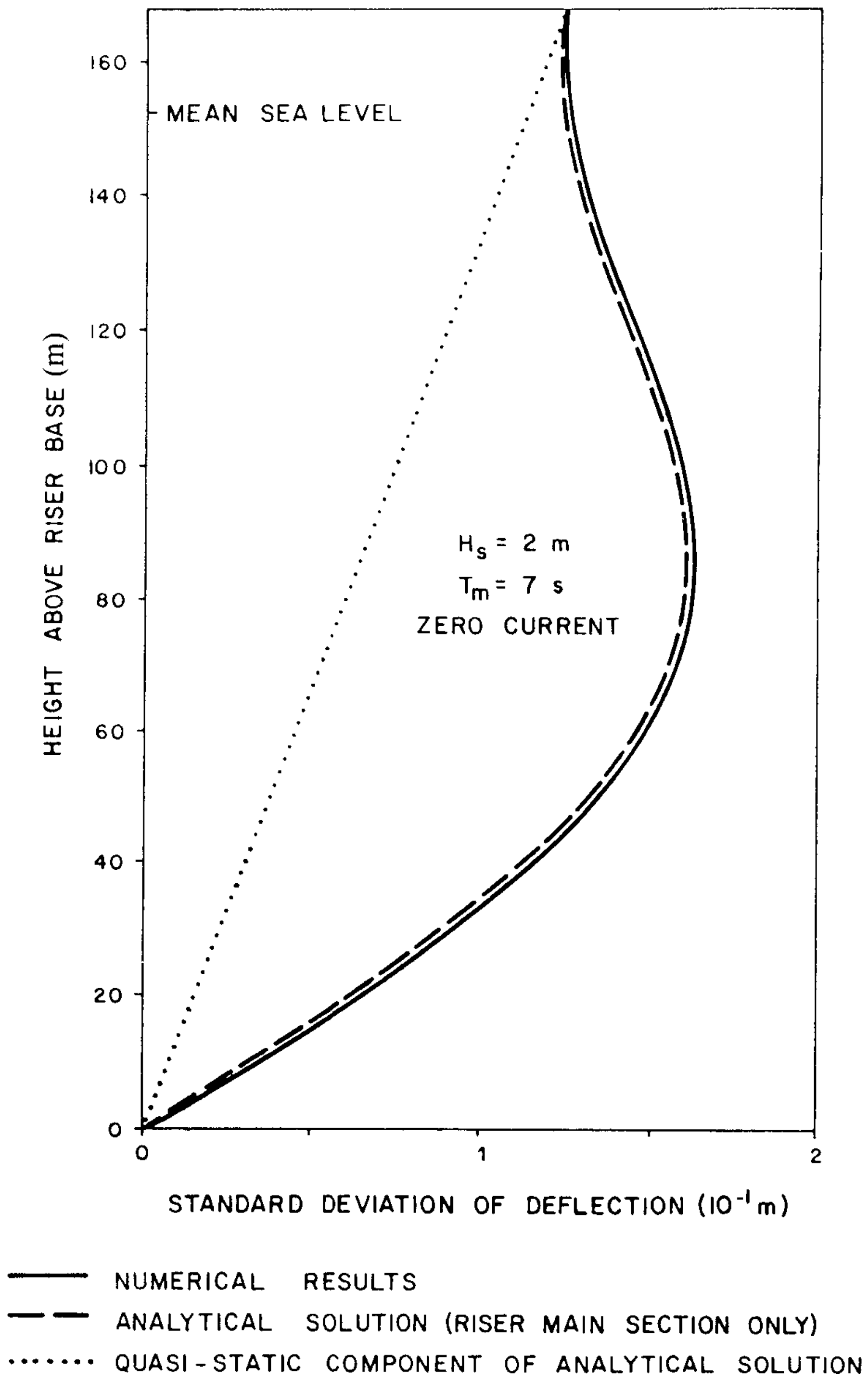

Fig. 6. Standard deviation of deflection versus height above riser base.

An entirely different type of response will occur when the damping forces are large as compared to the inertia forces: i.e. when the drag-inertia parameter δ, defined by equation (16), is large. As for linearly damped tensioned strings subject to transverse displacement excitation at one end, in this case the response will decay in magnitude from the top, over the characteristic distance λ_d, defined by equation (15). Maximum response will then occur at the top of the riser, i.e. in the wave-active zone, for which solutions have been given.

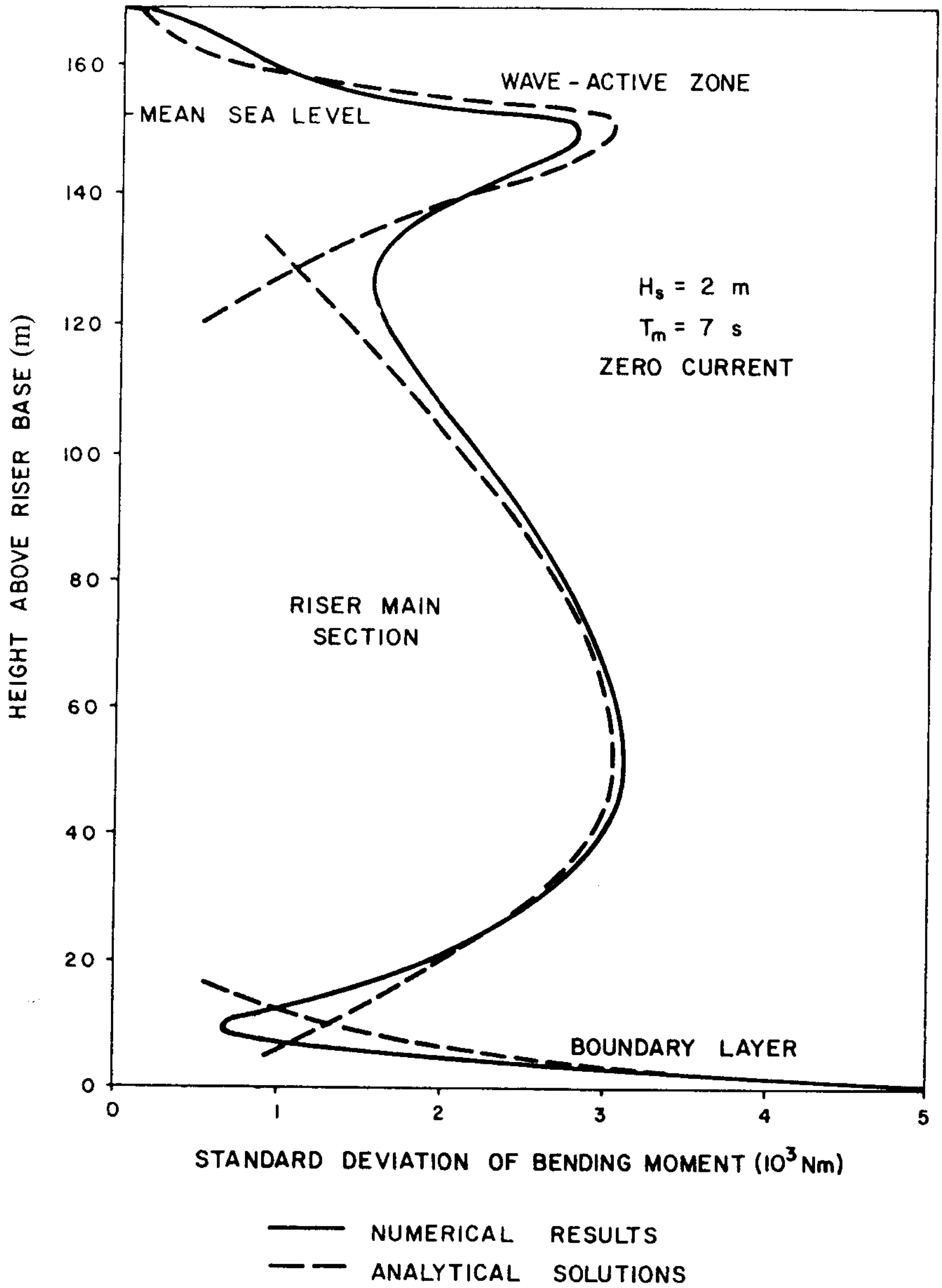

Fig. 7. Standard deviation of bending moment versus height above riser base.

NUMERICAL VERIFICATION OF ANALYTICAL SOLUTIONS

The power of the analytical methods given can be demonstrated by analysing the response of the multi-bore riser of a floating production system shown in fig. 5. The response of this riser to uni-directional random waves and floater motions has been calculated numerically using random time-domain simulation techniques: see Harper (1979). In the calculations, deflections, angles and curvatures of the central export riser and the peripheral flow lines were assumed to be the same. In this way, the riser could be modelled as a single tensioned beam. The hydrodynamic forces were described according to the relative velocity form of Morison's equation. A Pierson-Moskowitz spectrum, characterised by a significant wave height H_s and a mean period T_m, was assumed for the power spectral density of sea-surface elevation. Water particle velocities and accelerations were described according to a linear Gaussian model of the sea. Vessel motions correspond to those of a typical semi-submersible. Numerical results for the vertical distribution of standard deviation of riser deflection and riser bending moment obtained for a significant wave height H_s of 2 m, a mean period of the waves T_m of 7 s and zero current, are shown in figs. 6 and 7.

For the riser and environmental conditions under consideration, the characteristic lengths λ_w, λ_b and λ_m were calculated to be 12 m, 6 m and 155 m, respectively. This indicates that a distinction between a wave-active zone at the top, a boundary layer at the bottom and a riser main section is justified. Furthermore, the drag-inertia parameter δ, based on floater displacement, was approximately 0.1 and the first natural frequency approximately 0.8 rad/s. The dynamic component of the solution for response in the riser main section, given by equation (39), was therefore dominated by resonance in the first natural mode and could be calculated using the analytical methods given by Brouwers (1982). Analytical results thus obtained for the standard deviation of the deflection and bending moment in the riser main section have been plotted in figs. 6 and 7. Fig. 7 also shows analytical results for standard deviation of bending moment in the wave-active zone and in the boundary layer at the bottom, as obtained from solutions (25) and (32), respectively.

From fig. 6 it is noted that the analytical solutions for deflection in the riser main section and the numerical results for deflection are in close agreement over the entire riser. Effects of direct wave loading at the top and 'boundary layer' effects at the bottom are not directly apparent. This is in agreement with the analytical results given. From fig. 7 it can be seen that the analytical results for the bending moment in the wave-active zone, the boundary layer at the bottom and the riser main section agree reasonably well with the corresponding numerical solutions. Differences between numerical and analytical results in the wave-active zone can be ascribed to neglect of floater motion in solution (25). Differences between numerical and analytical results in the boundary layer at the bottom are due to omission of a 'lower order term' in solution (32). This lower order term describes adjustment of non-zero bending moment at the bottom of the main section and becomes significant, in comparison with the given solution, in the case of small rotational stiffness of the riser base.

Apart from standard deviations, comparisons between numerically and analytically calculated non-Gaussian probability distributions of response have also been made (e.g. Brouwers, 1982). Also here, numerical results, in general, confirm analytical predictions.

CONCLUDING REMARKS

The previous analysis has shown that it is possible to distinguish three characteristic regions along slender (tension-dominated) risers in deep water: a wave-active zone at the top, a boundary layer at the bottom and a main section in between. For each of these regions it is possible to give analytical solutions, in terms of known time- and position-dependent functions. These solutions, supported by numerical calculations where required, provide a comprehensive and economic means for predicting the important statistic parameters of random riser response, such as expected fatigue damage and expected extreme response. Furthermore, the closed-form nature of the solutions enables the influence of major parameters (water depth, diameter, wave height, etc.) on riser response to be determined. General trends in riser behaviour can thus be identified.

ACKNOWLEDGEMENT

The author is indebted to the Management of Shell Research BV for permission to publish this paper. Furthermore, he wishes to thank Dr. W. Visser and Ir. P.H.J. Verbeek of Koninklijke/Shell Exploratie en Produktie Laboratorium for their constructive criticism and valuable comments.

REFERENCES

Batchelor, G.K. – An Introduction to Fluid Dynamics, Cambridge Univ. Press, London (1967).

Borgman, L.E. – Statistical Models for Ocean Waves and Wave Forces, Advances in Hydroscience (ed. V.T. Chow), Academic Press, New York (1972), Vol. 8.

Brouwers, J.J.H. – Response near Resonance of Non-Linearly Damped Systems subject to Random Excitation with Application to Marine Risers, Ocean Engineering **9**, 235–257 (1982).

Harper, M.P. – Production Riser Analysis, Proc. 2nd BOSS Conference, Paper **60**, London (1979).

Hogben, N., B.L. Miller, J.W. Searle and G. Ward – Estimation of Fluid Loading on Offshore Structure, Proc. Instn. Civ. Engrs, Part 2, **63**, 515–562 (1977).

Kinsman, B. – Wind Waves, Prentice-Hall, Inc., New York (1965).

Kirk, C.L., E.U. Etok and M.T. Cooper – Dynamic and Static Analysis of a Marine Riser, Applied Ocean Research **1**, 125–135 (1979).

Krolikowsky, L.P. and T.A. Gay – An Improved Linearisation Technique for Frequency Domain Riser Analysis, Proc. 12th Annual Offshore Technology Conference, Paper 3777, Houston (1980).

Moe, G. and S.H. Crandall – Extremes of Morison-Type Wave Loading on a Single Pile, Trans. ASME, J. Mech. Design **100**, 100–104 (1978).

Pierson, W.J. Jr. and P. Holmes – Irregular Wave Forces on a Pile, J. Waterways and Harbors, Proc. Amer. Soc. Civil Eng. **91** (ww4), 1–10 (1965).

Sarpkaya, T. – A Critical Assessment of Morison's Equation, Proc. Int. Symp. Hydrodynamics in Ocean Engineering, Trondheim, Norway, **1**, 447–467 (1981)

Sexton, R.M. and L.K. Agbezuge – Random Wave and Vessel Motion Effects on Drilling Riser Dynamics, 8th Annual Offshore Technology Conference, Paper 2650, Houston (1976).
Tickell, R.G. – Continues Random Wave Loading on Structural Members, The Structural Engineer **55**, no. 5, 209–222 (1977).
Tucker, T.C. and J.P. Murtha – Non-Deterministic Analysis of a Marine Riser, Proc. 5th Annual Offshore Technology Conference, Paper 1770, Houston (1973).
Tung, C.C. – Peak Distribution of Random Wave-Current Force, Journal of the Engineering Mechanics Division, ASCE, EM5, 873–884 (1974).
Van Dyke, M. – Perturbation Methods in Fluid Mechanics, Academic Press, New York (1964).